STM JOURNALS

Journal of Experimental & Applied Mechanics
ISSN: 2230-9845 (Online), ISSN: 2321-516X (Print)
Volume 8, Issue 3
www.stmjournals.com

An Investigation of Stress and Deformation States of Rotating Functionally Graded Spherical Pressure Vessels

Amit Kumar Thawait[1,*], Lakshman Sondhi[2], Rupesh Kumar Verma[3], Prashant Kumar Jangde[1]

[1]Department of Mechanical Engineering, Institute of Technology, Guru Ghasidas Vishwavidyalaya, Bilaspur, Chhattisgarh, India

[2]Department of Mechanical Engineering, Shri Shankaracharya College of Engineering and Technology, Bhilai, Chhattisgarh, India

[3]Department of Mechanical Engineering, Rungta College of Engineering and Technology, Bhilai, Chhattisgarh, India

Abstract

The present study deals with the analysis of rotating spherical pressure vessels made of functionally graded materials (FGMs). Material properties are graded along the radial direction, which is achieved by varying volume fractions of the constituting materials according to Mori-Tanaka scheme. Shells are subjected to hydrostatic internal pressure and have free boundary condition at the outer surface. Governing equations are derived using principle of stationary total potential. The effects of grading parameter and thickness parameter on stress and deformation behavior of the shells are investigated for ceramic-metal shell. Results obtained show that there is a significant reduction in stresses and deformation of the FGM shells as compared to homogeneous shell.

Keywords: *Functionally graded material (FGM), elastic analysis, rotating spherical pressure vessel, Mori-Tanaka scheme*

****Author for Correspondence*** E-mail: amkthawait@gmail.com

INTRODUCTION

Functionally graded materials (FGMs) are special composite materials that have continuous variations of material properties. Properties are graded in a particular direction by varying the volume fractions of the constituent materials. Functionally graded shells are widely used in space vehicles, aircrafts, nuclear power plants and many other engineering applications [1]. It is very important to control and optimize stresses and displacement fields due to internal pressure and centrifugal force which is achieved by controlling the change in local material properties in FGMs.

Many researchers have worked on stress analysis of rotating spherical shells, conical shells, cylindrical shells, disks etc. by analytical as well as approximate methods. Tutuncu and Ozturk [2] found closed form solution for stresses and displacements in functionally graded cylindrical and spherical vessels subjected to internal pressure by using the infinitesimal theory of elasticity. The material stiffness obeying a power law is assumed to vary through the wall thickness and poisson's ratio is assumed constant. Alavi, Karimi, and Bagri [3] reported work on the thermoelastic behavior of thick functionally graded hollow sphere under thermal and mechanical loads. The mechanical and thermal properties of FG sphere are assumed to be functions of radial coordinates. Two methods were used to estimate the effective mechanical properties of functionally graded sphere. One is the Rule of Mixture (R-M) scheme and another is Mori-Tanaka scheme. Tutunku and Temel [4] analyzed displacements and stresses in axisymmetric geometries like functionally-graded hollow cylinders, disks and spheres subjected to uniform internal pressure. They used plane elasticity theory and complementary functions method and assumed that the material is functionally graded in the radial direction. Chen and Lin [5] reported an alternative solution for the problems of thick-walled cylinders and spheres of functionally graded materials (FGMs). They defined two fundamental solutions from a numerical solution under two particular initial boundary conditions.

They also defined the transmission matrix for the single layer as well as multi-layered shells which relates the values of radial stress and displacement at the initial point to those at the end point of the layer.

In recent work Anh, Bich, and Duc [6] worked on nonlinear stability analysis of thin annular spherical shells made of functionally graded materials (FGM) on elastic foundations under external pressure and temperature. Material properties are graded in the thickness direction according using a simple power law distribution in terms of the volume fractions of constituents. Kar and Panda [7] dealt with the linear and the nonlinear deformation analysis of functionally graded (FG) spherical shell panel under thermo-mechanical load. The temperature dependent effective material properties of FG shell panel are evaluated using Voigt's micro-mechanical rule in conjunction with power-law distribution. Tung [8] presented an analytical approach to analyze the nonlinear axisymmetric response of Functionally Graded (FG) Shallow Spherical Shells (SSSs) resting on elastic foundations which is exposed to thermal environment and subjected to uniform external pressure. Material properties are assumed to be temperature-independent and graded in the thickness direction according to a simple power law distribution in terms of the volume fractions of constituents.

In present research work rotating spherical pressure vessels under pressurized – free boundary condition is analyzed. Governing equations are derived by principle of stationary total potential. The shells are made of functionally graded material of aluminum metal and zirconia ceramic. Functional gradation of the material properties is done by Mori-Tanaka scheme. The effects of functional gradation of the material properties on the displacement and stresses of the shells for ceramic-metal FGM are presented. At the same time the effects of thickness parameter is also investigated and presented for some numerical problem.

MATERIAL MODELING

The effective bulk modulus and shear modulus of the FGM disk, evaluated using the Mori-Tanaka scheme are given by [9]:

$$B(r) = (B_o - B_i)/V_o\left(1+(1-V_o)\frac{3(B_o-B_i)}{3B_i+4G_i}\right)+B_i \quad (1)$$

$$G(r) = (G_o - G_i)/V_o\left(1+(1-V_o)\frac{(G_o-G_i)}{G_i+f_1}\right)+G_i \quad (2)$$

$$f_1 = \frac{G_i(9B_i+8G_i)}{6(B_i+2G_i)} \quad (3)$$

Here, V is the volume fraction of the phase material. The subscripts i and o refer to the inner and outer materials respectively. The volume fractions of the inner and outer phases are related by:

$$V_i + V_o = 1 \quad (4)$$

Where, V_o is expressed as

$$V_o = \left(\frac{x-1}{k-1}\right)^n \quad (5)$$

Where, $x = r/r_i$ and $k = r_o/r_i$, (which is a measure of thickness) n $(n \geq 0)$ is the volume fraction exponent. The elastic modulus E can be found as:

$$E(r) = \frac{9B(r)G(r)}{3B(r)+G(r)} \quad (6)$$

The mass density ρ can be given by the rule of mixtures as:

$$\rho(r) = (\rho_o - \rho_i)\left(\frac{r-r_i}{r_o-r_i}\right)^n + \rho_i \quad (7)$$

PROBLEM FORMULATION

Spherical shell is an axisymmetric body whose behavior is independent of coordinate θ of a cylindrical frame of reference (r, θ, z). Figure 1 shows the geometry of spherical vessel subjected to pressurized boundary condition at inner surface and free boundary condition at outer surface. Using quadratic quadrilateral element, the displacement vector $\{\varphi\}$ can be obtained as [10]:

$$\{\varphi\} = \{u \quad v\}^T = [N]\{\delta\}^e \quad (8)$$

Where, u and v are the components of displacement in radial and axial direction respectively, [N] is the matrix of quadratic shape functions and $\{\delta\}$ is the nodal displacement vector, given as:

$$[N] = \begin{bmatrix} N_1 & 0 & N_2 & 0 & \ldots. & N_8 & 0 \\ 0 & N_1 & 0 & N_2 & \ldots. & 0 & N_8 \end{bmatrix} \quad (9)$$

$$\{\delta\}^e = \{u_1 \quad v_1 \quad u_2 \quad v_2 \quad \ldots \quad \ldots \quad u_8 \quad v_8\}^T \quad (10)$$

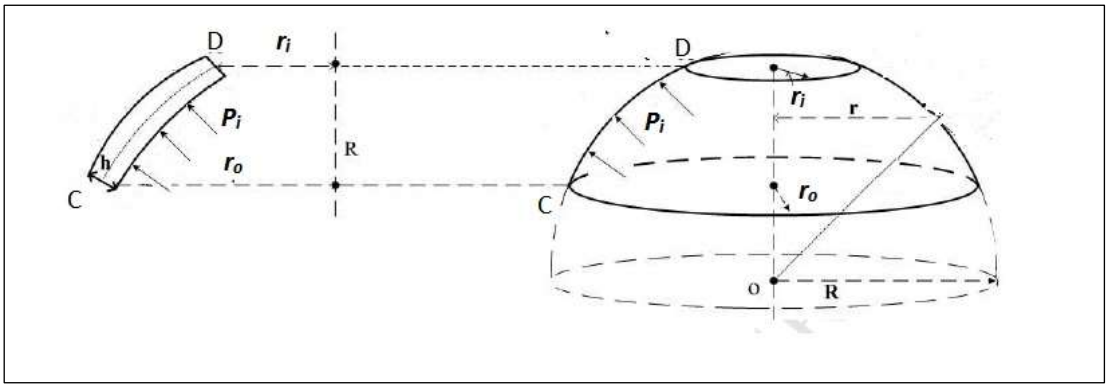

Fig. 1: *Geometry of Spherical Shell.*

Shape functions in natural coordinates are given as:

$$N_1 = \left(\frac{1}{4}\right)(1-\xi)(1-\eta)(-1-\xi-\eta) \qquad N_5 = \left(\frac{1}{2}\right)(1-\xi^2)(1-\eta)$$

$$N_2 = \left(\frac{1}{4}\right)(1+\xi)(1-\eta)(-1+\xi-\eta) \qquad N_6 = \left(\frac{1}{2}\right)(1+\xi)(1-\eta^2)$$

$$N_3 = \left(\frac{1}{4}\right)(1+\xi)(1+\eta)(-1+\xi+\eta) \qquad N_7 = \left(\frac{1}{2}\right)(1-\xi^2)(1+\eta)$$

$$N_4 = \left(\frac{1}{4}\right)(1-\xi)(1+\eta)(-1-\xi+\eta) \qquad N_8 = \left(\frac{1}{2}\right)(1-\xi)(1-\eta^2)$$

The strain components are related to elemental displacement components as:

$$\{\varepsilon\} = \{\varepsilon_r \quad \varepsilon_\theta \quad \varepsilon_z \quad \gamma_{rz}\}^T = \left\{\frac{\partial u}{\partial r} \quad \frac{u}{r} \quad \frac{\partial v}{\partial z} \quad \frac{\partial u}{\partial z} + \frac{\partial v}{\partial r}\right\}^T \tag{11}$$

$$\left\{\frac{\partial u}{\partial r} \quad \frac{u}{r} \quad \frac{\partial v}{\partial z} \quad \frac{\partial u}{\partial z} + \frac{\partial v}{\partial r}\right\}^T = [B_1] \times \left\{\frac{\partial u}{\partial r} \quad \frac{\partial u}{\partial z} \quad \frac{\partial v}{\partial r} \quad \frac{\partial v}{\partial z} \quad \frac{u}{r}\right\}^T \tag{12}$$

Where, ε_r, ε_θ, ε_z and γ_{rz} are radial, tangential, axial and shear strain respectively. By transforming the global coordinates into natural coordinates (ξ-η),

$$\left\{\frac{\partial u}{\partial r} \quad \frac{\partial u}{\partial z} \quad \frac{\partial v}{\partial r} \quad \frac{\partial v}{\partial z} \quad \frac{u}{r}\right\}^T = [B_2] \times \left\{\frac{\partial u}{\partial \xi} \quad \frac{\partial u}{\partial \eta} \quad \frac{\partial v}{\partial \xi} \quad \frac{\partial v}{\partial \eta} \quad \frac{u}{r}\right\}^T \tag{13}$$

$$\left\{\frac{\partial u}{\partial \xi} \quad \frac{\partial u}{\partial \eta} \quad \frac{\partial v}{\partial \xi} \quad \frac{\partial v}{\partial \eta} \quad \frac{u}{r}\right\}^T = [B_3] \times \{\delta\}^e \tag{14}$$

The above elemental strain-displacement relationships can be written as:

$$\{\varepsilon\} = [B]\{\delta\}^e \tag{15}$$

Where [*B*] is strain-displacement relationship matrix, which contains derivatives of shape functions. For a quadratic quadrilateral element, it is calculated as:

$$[B] = [B_1] \times [B_2] \times [B_3] \tag{16}$$

$$[B_1] = \begin{bmatrix} 1 & 0 & 0 & 0 & 0 \\ 0 & 0 & 0 & 0 & 1 \\ 0 & 0 & 0 & 1 & 0 \\ 0 & 1 & 1 & 0 & 0 \end{bmatrix} \tag{17}$$

$$[B_2]=\begin{bmatrix} \frac{J_{22}}{|J|} & \frac{-J_{12}}{|J|} & 0 & 0 & 0 \\ \frac{-J_{21}}{|J|} & \frac{J_{11}}{|J|} & 0 & 0 & 0 \\ 0 & 0 & \frac{J_{22}}{|J|} & \frac{-J_{12}}{|J|} & 0 \\ 0 & 0 & \frac{-J_{21}}{|J|} & \frac{J_{11}}{|J|} & 0 \\ 0 & 0 & 0 & 0 & 1 \end{bmatrix} \tag{18}$$

Where, J is the Jacobian matrix, used to transform the global coordinates into natural coordinates. It is given as:

$$[J]=\begin{bmatrix} \sum_{i=1}^{8}\frac{\partial N_i}{\partial \xi} r_i & \sum_{i=1}^{8}\frac{\partial N_i}{\partial \xi} z_i \\ \sum_{i=1}^{8}\frac{\partial N_i}{\partial \eta} r_i & \sum_{i=1}^{8}\frac{\partial N_i}{\partial \eta} z_i \end{bmatrix} \tag{19}$$

$$[B_3]=\begin{bmatrix} \frac{\partial N_1}{\partial \xi} & 0 & \frac{\partial N_2}{\partial \xi} & 0 & \dots & \dots & \frac{\partial N_8}{\partial \xi} & 0 \\ \frac{\partial N_1}{\partial \eta} & 0 & \frac{\partial N_2}{\partial \eta} & 0 & \dots & \dots & \frac{\partial N_8}{\partial \eta} & 0 \\ 0 & \frac{\partial N_1}{\partial \xi} & 0 & \frac{\partial N_2}{\partial \xi} & \dots & \dots & 0 & \frac{\partial N_8}{\partial \xi} \\ 0 & \frac{\partial N_1}{\partial \eta} & 0 & \frac{\partial N_2}{\partial \eta} & \dots & \dots & 0 & \frac{\partial N_8}{\partial \eta} \\ \frac{N_1}{r} & 0 & \frac{N_2}{r} & 0 & \dots & \dots & \frac{N_8}{r} & 0 \end{bmatrix} \tag{20}$$

From generalized Hooks law, components of stresses in radial, tangential and axial direction (σ_r, σ_θ, σ_z and τ_{rz}) are related to components of total strain as:

$$\varepsilon_r=\frac{1}{E}\left(\sigma_r-\nu\sigma_\theta-\nu\sigma_z\right) \tag{21}$$

$$\varepsilon_\theta=\frac{1}{E}\left(\sigma_\theta-\nu\sigma_r-\nu\sigma_z\right) \tag{22}$$

$$\varepsilon_z=\frac{1}{E}\left(\sigma_z-\nu\sigma_\theta-\nu\sigma_r\right) \tag{23}$$

In generalized matrix notation, stress-strain relation can be written as:

$$\{\sigma\}=\left[D(r)\right]\{\varepsilon\} \tag{24}$$

Where, $D(r)$ is stress-strain relationship matrix and is a function of radius r.

$$\{\sigma\}=\{\sigma_r \quad \sigma_\theta \quad \sigma_z \quad \tau_{rz}\}^T \tag{25}$$

$$D(r)=\frac{(1-\nu)E(r)}{(1+\nu)(1-2\nu)}\begin{bmatrix} 1 & \frac{\nu}{(1-\nu)} & \frac{\nu}{(1-\nu)} & 0 \\ \frac{\nu}{(1-\nu)} & 1 & \frac{\nu}{(1-\nu)} & 0 \\ \frac{\nu}{(1-\nu)} & \frac{\nu}{(1-\nu)} & 1 & 0 \\ 0 & 0 & 0 & \frac{1-2\nu}{2(1-\nu)} \end{bmatrix} \tag{26}$$

$$\{\varepsilon\}=\{\varepsilon_r \quad \varepsilon_\theta \quad \varepsilon_z \quad \gamma_{rz}\}^T \tag{27}$$

When the shell rotates, it experiences a distributed force over its volume. Under these forces when shell is properly supported, it undergoes deformation and stores internal strain energy *U*, which is given by:

$$U=\frac{1}{2}\int_V \{\varepsilon\}^T\{\sigma\}\, dv \tag{28}$$

The potential of external body and surface force is given by:

$$W=-\int_V \{\delta\}^T\{q_v\}\, dv-\int_S \{\delta\}^T\{q_s\}\, ds \tag{29}$$

Using Eqs. (15) and (24) the element level equations can be obtained as:

$$U^e=\int_V \{\delta\}^{eT}[B]^T[D(r)][B]\{\delta\}^e\, \pi r dr dz \tag{30}$$

$$W^e=-\int_V 2\{\delta\}^{eT}[N]^T\{q_v\}\pi r dr dz-\int_S \{\delta\}^{eT}[N]^T\{q_s\}\, dr dz \tag{31}$$

The total potential of the element can be written as:

$$\pi_p{}^e=\int_V \{\delta\}^{eT}[B]^T[D(r)][B]\{\delta\}^e\, \pi r dr dz-\int_V 2\{\delta\}^{eT}[N]^T\{q_v\}\pi r dr dz-\int_S \{\delta\}^{eT}[N]^T\{q_s\}\, dr dz \tag{32}$$

Defining element stiffness matrix $[K]^e$ and element load vector $\{f\}^e$ as:

$$[K]^e=2\int_V [B]^T[D(r)][B]\, \pi r dr dz \tag{33}$$

$$\{f\}^e=2\int_V \{\delta\}^{eT}[N]^T\{q_v\}\pi r dr dz+\int_S \{\delta\}^{eT}[N]^T\{q_s\}\, dr dz \tag{34}$$

Transforming global coordinates into natural coordinates:

$$[K]^e=2\pi\int_{-1}^{1}\int_{-1}^{1}[B]^T[D(r)][B] r|J|\, d\xi d\eta \tag{35}$$

$$\{f\}^e=2\pi\int_V \{\delta\}^{eT}[N]^T\{q_v\} r|J|\, d\xi d\eta+\int_S \{\delta\}^{eT}[N]^T\{q_s\}|J|\, d\xi d\eta \tag{36}$$

Multilayer modeling of the geometry gives singular field variables at the boundaries of the glued areas. Therefore to assign the average material properties to the elements of mesh of the single geometry is a better approach. In other words it means assigning material properties to the finite elements instead of geometry. In Eq. (24), the [*D*(*r*)] matrix, is a function of *r*, which is calculated numerically at each node, which results into continuous material property distribution throughout the geometry. This is due to the fact that the shape functions in the elemental formulations being coordinate functions make it easier to implement the same [11].

$$\phi^e = \sum_{i=1}^{8} \phi_i N_i \tag{37}$$

Where ϕ^e is element material property, ϕ_i is material property at node i and N_i is the shape function. Where, J is the Jacobian matrix, which is given by Eq. (19). Total potential energy of the shell is given by:

$$\pi_p = \sum \pi_p^{\ e} \tag{38}$$

Using the principle of stationary total potential (PSTP) the total potential is set to be stationary with respect to small variation in the nodal degree of freedom that is:

$$\frac{\partial \pi_p}{\partial \{\delta\}^T} = 0 \tag{39}$$

Which gives system level equation for shell as:

$$[K]\{\delta\} = \{F\} \tag{40}$$

Where,

$$[K] = \sum_{n=1}^{N} [K]^e = Globel\ Stiffness\ matrix$$

$$\{F\} = \sum_{n=1}^{N} [f]^e = Globel\ load\ vector$$

RESULTS AND DISCUSSION

Validation

To validate the current work, problems of reference [4] are reconsidered and two types of material models are analyzed. Following equations are used for material modelling:

$$V_c = \left(\frac{x-1}{k-1}\right)^n \tag{41}$$

$$\nu = \nu_c V_c + \nu_m (1 - V_c) \tag{42}$$

$$E = E_c V_c + E_m (1 - V_c) \tag{43}$$

Where, V is the volume fraction, E is young's modulus and v is Poisson's ratio, subscript 'm' refers to metal and 'c' refers to ceramic. x is non-dimensional radius that is r/a and k is the ratio of outer diameter to inner diameter that is b/a, where a and b are inner and outer radius respectively.

In model 1, Poisson's ratio is taken constant (0.333) and Young's modulus varies according to Eq. (40) taking n=1, while in model 2, both Poisson's ratio and Young's modulus vary according to Eqs. (40) and (41) taking n=k=2. Material properties of the metal and ceramic used are: E_m=200 *GPa*, E_c=360 *GPa*, ν_m=0.333, ν_c=0.2 and the vessels are subjected to unit internal pressure that is 1 *GPa*.

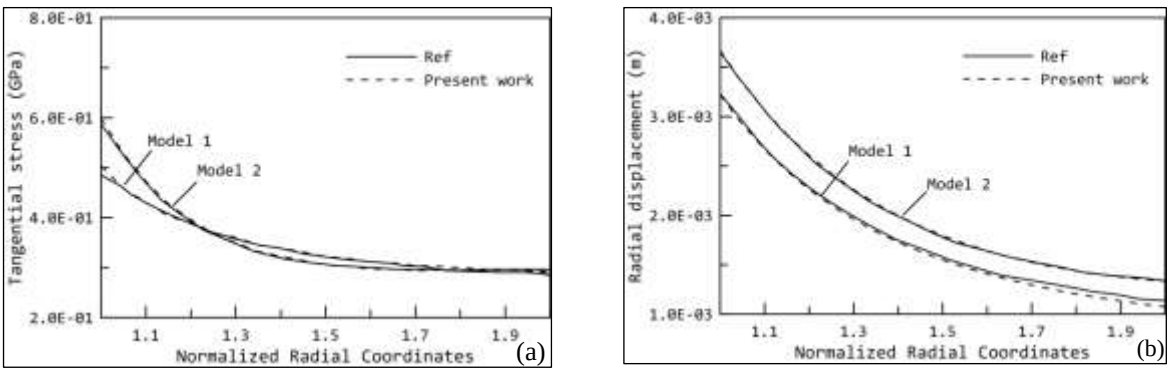

Fig. 2: *Comparison of the results of the current work with Reference; (a)Tangential stress (b) Radial displacement [4].*

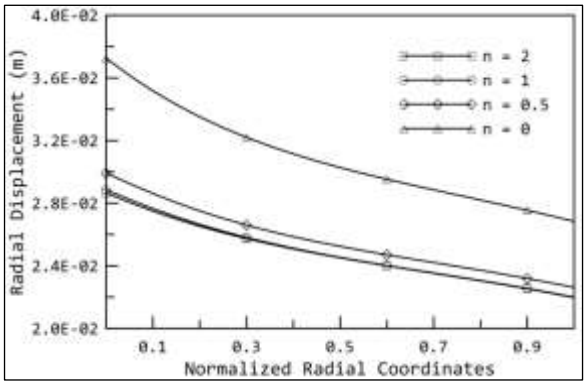

Fig. 3: *Distribution of Radial Displacement for Different values of n.*

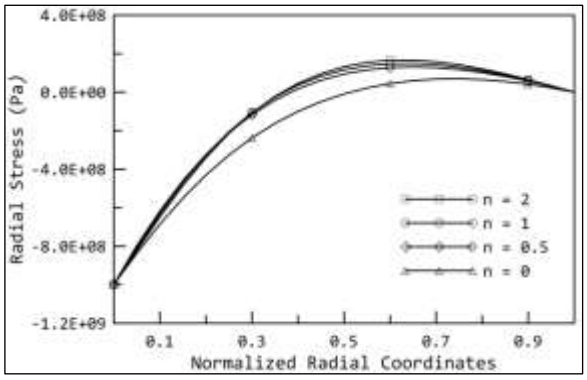

Fig. 4: *Distribution of Radial Stress for Different values of n.*

Figure 2(a) and (b) show the comparison of tangential stress and radial displacement with the results of reference respectively. It can be seen that both the results are in good agreement.

Numerical Results

Figures 3–6 show the distribution of radial displacement, radial stress, tangential stress and von Mises stress respectively for different values of grading parameter *n* taking *k*=2; while Figures 7–10 show the same distributions for different values of parameter *k* taking *n*=1. Shells are rotating with an angular velocity of 500 *rad/s*, subjected to unit internal pressure that is 1 *GPa*. Material is modeled by Mori-Tanaka scheme for which aluminium metal at outer surface and zirconia ceramic at inner surface is taken. Properties of aluminium and zirconia are as in Table 1 [9]: where *B* and *G* denote bulk modulus and shear modulus respectively.

Table 1: *Material properties of the constituent materials.*

Material	*E* (GPa)	ρ (kg/m^3)	*B*(*GPa*)	*G*(*GPa*)	*v*
Aluminum	70	2700	58.333	26.9231	0.3
Zirconia	151	5700	128.333	58.0769	0.3

From Fig. 3 it can be seen that FGM shell having $n = 0$ has maximum radial displacement while the FGM shell having $n = 2$ has minimum radial displacement. $n = 0$ indicates homogeneous shell made of outer material that is material at $r = r_o$. Radial displacement is minimum at the outer surface and maximum at the inner surface for all the shells. It is observed that radial displacement decreases with an increase in grading index *n*. Increasing *n* means volume fraction of the outer material (metal) is decreasing and inner material (ceramic) is increasing, which decreases radial displacement.

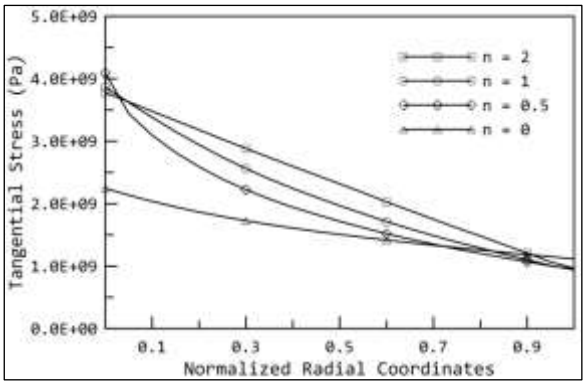

Fig. 5: *Distribution of Tangential Stress for Different values of n.*

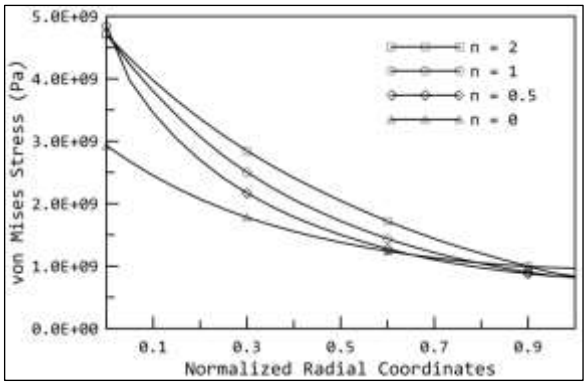

Fig. 6: *Distribution of von Mises Stress for Different values of n.*

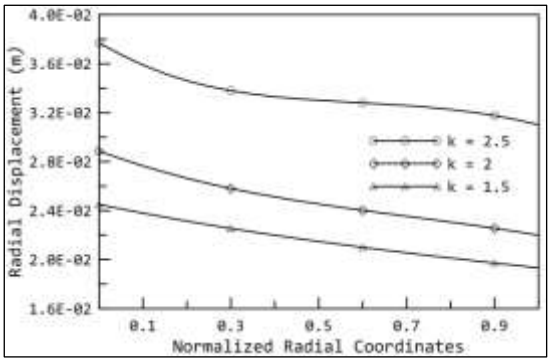

Fig. 7: *Distribution of Radial Displacement for Different values of k.*

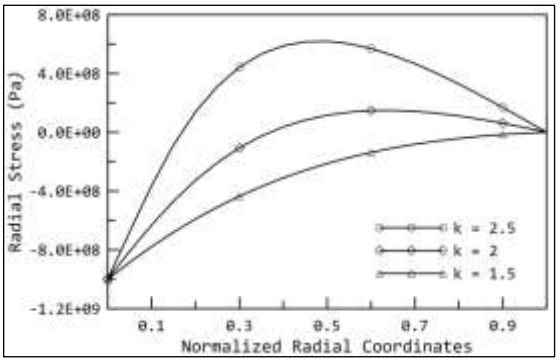

Fig. 8. *Distribution of Radial Stress for Different values of k.*

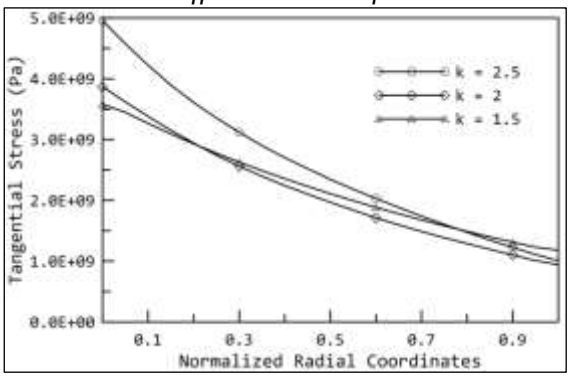

Fig. 9: *Distribution of Tangential Stress for Different values of k.*

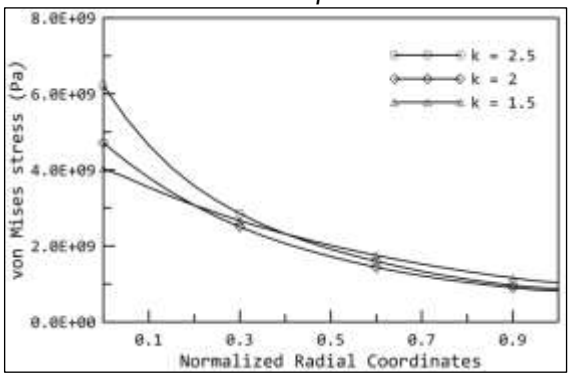

Fig. 10: *Distribution of von Mises Stress for Different values of k.*

From Figure 4, it is observed that radial stress is zero at the outer surface and maximum (equal to applied pressure) at the inner surface, which confirms the pressurized-free boundary condition applied on it. Radial stress is tensile and compressive both in nature but compressive stress is more as compared to tensile stress. Tensile nature increases with increasing *n.* FGM having grading parameter *n* = 2 has maximum tensile stress while FGM shell having value of grading parameter *n* = 0 has maximum compressive stress. Tangential stress and von Mises stress both have same distribution pattern. Both are completely tensile and increases with increasing value of n due to increasing ceramic content in FGM. Homogeneous metallic shell has minimum tangential and von Mises stress and FGM shell having grading index n = 2 has the maximum tangential and von Mises stress.

From Figure 7, it can be seen that shell having *k*=1.5 has minimum radial deformation and *k*=2.5 has maximum radial deformation. Therefore radial deformation increases with increasing value of parameter *k*. Radial stress is tensile and compressive both. Tensile radial stress is maximum for *k*=2.5 while compressive radial stress is maximum for *k*=1.5. Tangential stress and von Mises stress both are tensile only and *k*=1.5 has minimum tangential and von Mises stress.

By comparing all the stresses it can be seen that von Mises stress is maximum for all values of grading index *n* and *k* as compared to radial and tangential stress. Therefore von Mises stress should be taken as stress criteria to design rotating spherical pressure vessels. Further it is observed that FGM shell having grading parameter *n*=0 and *k=1.5* has the minimum von Mises stress; but n = 0 has highest deformation; therefore it is suggested to use the value of *n* in between 0 to 1 and *k* = 1.5 for designing rotating spherical pressure vessel.

CONCLUSION

The present work proposes a study of rotating FGM spherical pressure vessel based on principle of stationary total potential. The effect of gradation of material properties on

stress and deformation states is investigated and presented in the form of graph for different values of grading parameter *n* and parameter *k*. The results obtained are found to be in good agreement with established reports. It is observed that there is a significant reduction in stresses and deformation behavior of the FGM shell as compared to homogeneous shell. It is suggested that ceramic-metal FGM shell having n between 0 to 1 and k = 1.5 can be most effectively employed for the purpose of rotating spherical pressure vessels.

REFERENCES

1. Nejad MZ, Jabbari M, Ghannad M. Elastic Analysis of FGM Rotating Thick Truncated Conical Shells with Axially-Varying Properties under Non-Uniform Pressure Loading. *Compos Struct*. 2015; 122: 561–569p.
2. Tutuncu N, Ozturk M. Exact Solutions for Stresses in Functionally Graded Pressure Vessels. *Compos Part B.* 2001; 32: 683–686p.
3. Alavi F, Karimi D, Bagri A. An Investigation on Thermoelastic Behaviour of Functionally Graded Thick Spherical Vessels under Combined Thermal and Mechanical Loads. *Journal of Achievements in Materials and Manufacturing Engineering*. 2008; 31: 422–428p.
4. Tutunku N, Temel B. A Novel Approach to Stress Analysis of Pressurized FGM Cylinders, Disks and Spheres. *Compos Struct*. 2009; 91: 385–390p.
5. Chen YZ, Lin XY. An Alternative Numerical Solution of Thick-Walled Cylinders and Spheres Made of Functionally Graded Materials. *Comput Mater Sci*. 2010; 48: 640–647p.
6. Anh VTT, Bich DH, Duc ND. Nonlinear Stability Analysis of Thin FGM Annular Spherical Shells on Elastic Foundation under External Pressure and Thermal Loads. *Eur J Mech A Solids.* 2014; 50: 28–38p.
7. Kar VR, Panda SK. Nonlinear Thermomechanical Deformation Behaviour of P-FGM Shallow Spherical Shell Panel. *Chin J Aeronaut*. 2015; 29: 173–183p.
8. Tung HV. Non-Linear Axisymmetric Response of FGM Shallow Spherical Shells with Tangential Edge Constraints and Resting on Elastic Foundations. *Compos Struct*. 2016; 149: 231–238p.
9. Bayat M, Sahari BB, Saleem M, *et al.* Analysis of Functionally Graded Rotating Disks with Parabolic Concave Thickness Applying an Exponential Function and the Mori-Tanaka Scheme. *IOP Conf. Series: Materials Science and Engineering*. 2011; 17: 1–11p.
10. Seshu P. *A Text Book of Finite Element Analysis.* PHI Learning Pvt. Ltd.; 2003.
11. Kim JH, Paulino GH. Isoparametric Graded Finite Elements for Non-Homogeneous Isotropic and Orthotropic Materials. *ASME J Appl Mech*. 2002; 69: 502–514p.

Cite this Article
Amit Kumar Thawait, Lakshman Sondhi, Rupesh Kumar Verma and Prasant Kumar Jangde. An Investigation of Stress and Deformation States of Rotating Functionally Graded Spherical Pressure Vessels. *Journal of Experimental & Applied Mechanics*. 2017; 8(3): 19–27p.